RESEARCH PAPER

Transcription 5, e28869; May; © 2014 Landes Bioscience

Activation and reactivation of the RNA polymerase II trigger loop for intrinsic RNA cleavage and catalysis

Pavel Čabart[1], Huiyan Jin[1], Liangtao Li[2] and Craig D Kaplan[1,*]

[1]Department of Biochemistry and Biophysics; Texas A&M University; College Station, TX; [2]Department of Pathology; University of Utah School of Medicine; Salt Lake City, UT USA

Keywords: gene expression, general transcription factors, intrinsic cleavage, RNA synthesis, trigger loop

In addition to RNA synthesis, multisubunit RNA polymerases (msRNAPs) support enzymatic reactions such as intrinsic transcript cleavage. msRNAP active sites from different species appear to exhibit differential intrinsic transcript cleavage efficiency and have likely evolved to allow fine-tuning of the transcription process. Here we show that a single amino-acid substitution in the trigger loop (TL) of *Saccharomyces* RNAP II, Rpb1 H1085Y, engenders a gain of intrinsic cleavage activity where the substituted tyrosine appears to participate in acid-base chemistry at alkaline pH for both intrinsic cleavage and nucleotidyl transfer. We extensively characterize this TL substitution for each of these reactions by examining the responses RNAP II enzymes to catalytic metals, altered pH, and factor inputs. We demonstrate that TFIIF stimulation of the first phosphodiester bond formation by RNAP II requires wild type TL function and that H1085Y substitution within the TL compromises or alters RNAP II responsiveness to both TFIIB and TFIIF. Finally, Mn^{2+} stimulation of H1085Y RNAP II reveals possible allosteric effects of TFIIB on the active center and cooperation between TFIIB and TFIIF.

Introduction

Structurally and mechanistically conserved multi-subunit RNA polymerases (msRNAPs) drive RNA synthesis in all kingdoms of life. msRNAPs have likely evolved to attain a level of fidelity in transcript synthesis that balances error and synthesis rates. During the course of transcription, the msRNAP active center undertakes the nucleotide addition cycle (NAC), wherein substrates are selected, phosphodiester bond formation is catalyzed, and the enzyme translocates one nucleotide downstream to allow a repeat of the cycle. Outside of the NAC, msRNAPs also participate in additional factor-stimulated[1] or intrinsic RNA cleavage reactions that can contribute to transcription fidelity.[2-6]

Reactions in the msRNAP active site are generally promoted by a highly conserved and flexible domain called the trigger loop (TL), which is essential for efficient NTP substrate selection and catalysis.[7,8] Reactions promoted by the TL include the reverse reaction from phosphodiester bond formation, pyrophosphorolysis, and intrinsic cleavage of the RNA transcript (for some msRNAPs such as prokaryotic RNAP and eukaryotic RNAP II). Alternatively, RNAP I and RNAP III possess subunits that promote cleavage of RNA independently of the TL. The TL comprises two α-helices and a flexible region. Upon folding, specific residues in the flexible region attain helical character, and this transition can be observed in some msRNAP crystal structures where a matched NTP substrate is present and positioned in the active center. The TL is proposed to undergo cycles of movement/folding that underpin the opening and closing of the polymerase active site. As observed in structural studies, when the TL is in the closed conformation, NTP substrates can be trapped in the active center and a number of TL-NTP interactions are present. Highly conserved TL residues recognize different features of a correctly base-paired NTP substrate. The TL can be observed in a number of conformations, including partially folded states, and genetic experiments are consistent with a model for stepwise TL folding upon substrate interaction[9] (as reviewed by Kaplan in ref. 10). Translocation of msRNAPs is thought to be inhibited when the TL is closed, and movement of the TL into open conformation(s) has been proposed to allow translocation of the enzyme.[11-14]

Mutational studies in a number of systems have confirmed the importance of TL residues for substrate selection (matched vs. mismatched substrates, discrimination of NTPs from 2′-dNTPs) and efficient catalysis.[15-18] The TL has been proposed to directly contribute to catalysis through an absolutely conserved histidine *Saccharomyces cerevisiae* (*Sce*) Rpb1 H1085, *Escherichia coli* (*Eco*) β′ H936, *Thermus aquaticus* (*Taq*) β′ H1242).[7,19,20] This histidine is able to interact with the NTP β-phosphate and has been proposed to function as a general acid through donation of a proton to the pyrophosphate leaving group during nucleotidyl transfer.[7,19] Such a function for a positively charged residue may be widely present in nucleic acid polymerases,[19] and is supported

*Correspondence to: Craig D Kaplan; Email: cdkaplan@tamu.edu
Submitted: 03/08/14; Revised: 04/10/14; Accepted: 04/12/14; Published Online: 05/06/14
Citation: Čabart P, Jin H, Li L, Kaplan CD. Activation and reactivation of the RNA polymerase II trigger loop for intrinsic RNA cleavage and catalysis. Transcription 2014; 5:e28869; PMID: 24802894; http://dx.doi.org/10.4161/trns.28869

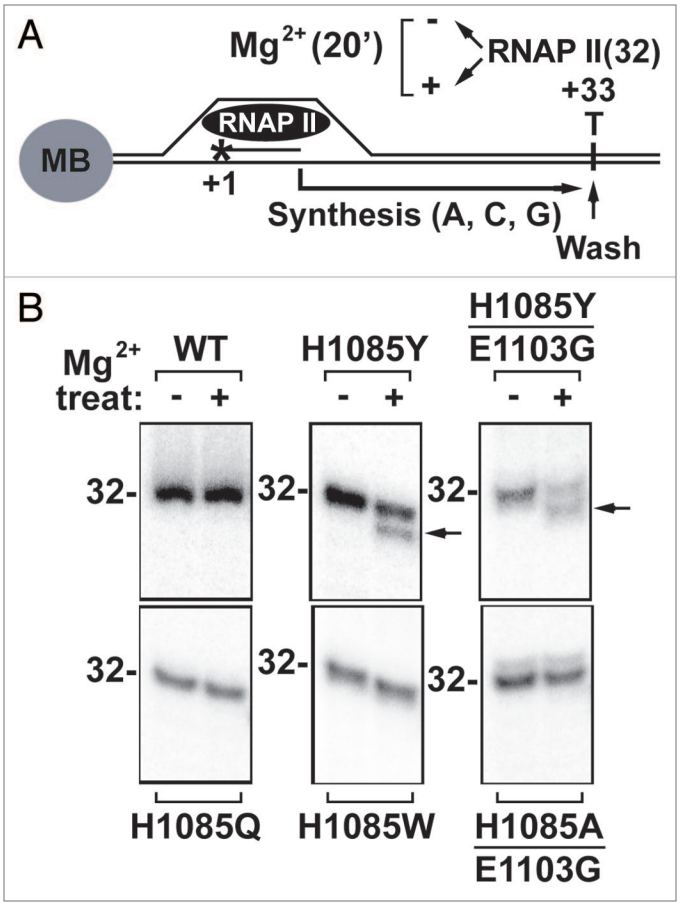

Figure 1. A single amino acid substitution of tyrosine for histidine within the TL at Rpb1 position 1085 activates intrinsic RNA cleavage. (**A**) Scheme of transcription and cleavage reactions on a 5′-end immobilized template. Scaffold-assembled 5′ ^{32}P-labeled 9-mer RNA with purified RNAP II was advanced with ATP, CTP and GTP to the T33 stop through omission of UTP, resulting in a radiolabeled 32-mer. These stalled elongation complexes (EC32) were washed to remove NTPs, and then challenged with Mg^{2+} ions or buffer in the absence of divalent cations. (**B**) Gain-of-function intrinsic cleavage activity is specific to H1085Y and H1085Y/E1103G RNAP II enzymes. Arrows indicate the RNA cleavage products. Experiments shown are representative of at least two independent determinations.

by computational simulations of the RNAP II transcription reaction,[21] though there are complexities to such simulations (for review see refs. 22, 23). Studies of pH effects on TL histidine-to-alanine substituted *Taq* RNAP, however, have failed to provide evidence for H1242 as a general acid due to the absence of any inhibition of elongation with increasing pH.[17] Such inhibition would have provided evidence for an alkaline titratable group in the reaction. The closed RNAP active site is predicted to become dehydrated,[24] which may have important (although difficult to predict) consequences on pK_as of critical residues.[23] Acid-base catalysis through this histidine is not essential for TL function because deletion of the TL generally has much greater effects on transcription than substitution of the histidine.[17,18,20] Importantly, however, individual substitutions in RNAPs of different species of highly conserved residues exhibit a wide ranges of effects, suggesting similar active centers can be distinctly shaped by evolution in different enzymes.[8,9,14,17,18] Therefore, the question remains open as to whether the conserved TL histidine functions as a general acid for RNAP II or other msRNAP active centers in RNA synthesis.

Cleavage activity by msRNAPs takes two major forms: an intrinsic cleavage activity, and a factor-stimulated cleavage activity. Similar to the differential contributions to transcription of conserved TL residues in different species, intrinsic cleavage of RNA substrates by the conserved active sites of msRNAPs can be wide-ranging. For example, *Sce* RNAP II possesses a very low RNA intrinsic cleavage ability in comparison to bacterial *Taq* and *Eco* RNAPs.[25,26] Even between these prokaryotic species there are large differences in reaction efficiency. *Taq* RNAP exerts an up to 100-fold increased activity when compared with *Eco* RNAP.[26-28] The role of the TL in intrinsic RNA hydrolysis is not completely clear in bacteria (see Zhang et al.[8]), and in eukaryotes intrinsic cleavage in the presence of α-amanitin has been observed.[4,5] As α-amanitin functions through restraint of the TL,[15,29] some intrinsic cleavage may be hypothesized to be TL-independent. Yuzenkova and Zenkin recently reported the essential role for the *Taq* β′ H1242 TL residue in intrinsic cleavage.[27] Two possible mechanisms were proposed. First, *Taq* H1242 may directly participate in the cleavage reaction by functioning as a general base to activate an attacking water molecule. Second, this histidine might orient the 3′-NMP, which itself consequently facilitates cleavage.[27] These different mechanisms may both be relevant, depending on the nature of the 3′-NMP participating in the intrinsic cleavage reaction, which has been termed "transcript-assisted transcriptional proofreading" for *Taq* RNAP. In this cleavage mode, it was proposed that the 2nd phosphodiester bond is almost exclusively cleaved at the 3′ end of RNA transcript within 1-bp backtracked and pretranslocated elongation complexes.[26] For *Eco* RNAP, the cleavage modes for removing a single NMP (exonuclease mode) and more than one NMP (endonuclease modes) have different requirements, underscoring the diversity among reactions within even a single enzyme.[28]

The TL is not required for factor-stimulated RNA cleavage; indeed, auxiliary cleavage factors (TFIIS in eukaryotes, GreA/B in bacteria) and related regulatory factors displace the TL away from the active center.[30] Generally, both intrinsic and factor-stimulated reactions use a two-metal ion mechanism and require proton transfers, likely supported by acid-base catalysis.[31] Different catalytic cations have distinct effects on msRNAP activities, and therefore may be used as probes for catalytic reactions. Two other divalent metals, Mn^{2+} and Co^{2+}, in addition to natively used Mg^{2+}, can support msRNAP catalysis as well as RNA hydrolysis.[32] The relative inability of yeast RNAP II to hydrolyze RNA was observed in the presence of Mg^{2+},[25] while Mn^{2+} and Co^{2+} were observed to be stimulatory for cleavage within some yeast elongation complexes (ECs).[4] Alternative catalytic cations also disrupt fidelity of nucleic acid polymerases for a number of enzymes. For example, Mn^{2+} and Cd^{2+} (the latter in the presence of Mg^{2+}) increased nucleotide misincorporation in *E. coli*.[32] A correlation between fidelity and the ability of a

metal ion to stimulate initiation of RNA synthesis while inhibiting elongation has been suggested.[33]

While the auxiliary cleavage factors and structurally-related regulatory factors noted above displace the TL, other transcription regulatory factors may conceivably function to control the TL or collaborate with it. RNAP II general transcription factors (GTFs) function to promote specific RNAP II initiation from promoters. For example, GTFs aid in RNAP II recruitment to specific locations and in opening ("melting") the DNA template for its insertion into the RNAP II active site (for recent reviews see refs. 34, 35). GTFs may also function in collaboration with the RNAP II active center subsequent to recruitment and template opening,[36] yet these functions are less well understood. It is unknown whether or how GTFs, specifically TFIIF and TFIIB, function in conjunction with the RNAP II TL or how they might influence RNAP II activity.

In this work we describe new findings indicating plasticity in mechanisms for intrinsic cleavage of RNA by msRNAPs; specifically, a novel cleavage activity exhibited by a mutant in the absolutely conserved *S. cerevisiae* RNAP II TL residue H1085 in conjunction with the RNA 3′-end. Our experiments reveal that the H1085Y substitution alters enzymatic function in multiple ways in response to pH and metal cofactor. We also find that the TL appears to cooperate with RNAP II GTFs in the formation of initial RNA synthesis products. The origin of a new activity in an otherwise highly constrained and conserved enzymatic active site nicely illustrates the possibility for unexpected changes providing raw material for the diversification of enzyme families. Taken together, this work extends the paradigm of the TL being a highly flexible and dynamic element central to multiple facets of msRNAP transcription.

Results

***Saccharomyces cerevisiae* H1085Y RNA polymerase II acquires a strong intrinsic cleavage activity**

In contrast to bacterial msRNAPs or RNAP I or RNAP III, yeast RNAP II exhibits weak intrinsic transcript cleavage activity.[25] Our previous work showed that H1085Y exhibited reduced transcription activity, with other substitutions in H1085 showing similar defects in vitro and similar phenotypes as H1085Y in vivo, with some differences in severity.[9,15] In vitro transcription reactions indicated that H1085Y conferred a unique intrinsic cleavage activity (**Fig. 1**). Stalled WT RNAP II elongation complexes treated with catalytic Mg^{2+} ion (**Fig. 1A**) exhibit no shortening of nascent transcript (**Fig. 1B**), consistent with a lack of efficient intrinsic transcript cleavage. In contrast, H1085Y RNAP II complexes exhibited a Mg^{2+}-dependent transcript shortening. The observed intrinsic cleavage was unique to H1085Y RNAP II among tested H1085 RNAP II substitution mutants. The elongation rate defects of H1085Y or other H1085 substituted RNAP II enzymes, as well as all observed in vivo phenotypes, could be at least partially suppressed by combination of H1085 substitutions with an additional RNAP II TL substitution, E1103G.[9,14,37] E1103G has been demonstrated to increase RNAP II catalytic activity while altering RNAP II translocation properties,[14,15,38] likely through promoting closure of the TL and trapping substrates in the active center.[16,39] In contrast to E1103G effects on all other previously observed H1085Y defects and phenotypes, the combination of E1103G with H1085Y did not result in suppression of the apparent H1085Y intrinsic cleavage activity. This result is consistent with RNA cleavage in H1085Y being a gain of function conferred by this mutation.

Requirements for the H1085Y cleavage reaction indicate novel properties

In order to understand the H1085Y intrinsic cleavage reaction, we examined its dependence on metal cofactor, sensitivity to pH and requirements for chemical groups on the 3′-end of the transcript, which are all factors implicated in RNAP intrinsic RNA cleavage. Although generally inefficient, yeast WT RNAP II intrinsic cleavage has been reported to be most active using Co^{2+} as a cofactor, followed by Mn^{2+}, and finally Mg^{2+} as the least active cofactor.[4] We confirmed these observations in our system (**Fig. S1**). In contrast to WT RNAP II, we found strong stimulation of the H1085Y reaction by Mn^{2+} (**Fig. 2A-2C**). Transcript cleavage patterns for H1085Y demonstrated moderate cleavage with Mg^{2+} (lane 3), followed by strong stimulation by Mn^{2+} or Co^{2+} (**Fig. 2C** lanes 4 and 5, respectively). In addition, a second RNA cleavage product of increased mobility appeared with Mn^{2+} treatment. We next examined whether the elongation complexes having undergone cleavage were maintained in a catalytically active state (**Fig. 2C**, lanes 6–8). Indeed, the addition of ATP, the specified base subsequent to the apparent cleavage position, allowed H1085Y RNAP II to extend the cleaved RNA to the original stall position.

As alkaline pH has been reported to stimulate intrinsic cleavage by WT RNAP II,[4,6] we assessed the pH-dependence of H1085Y intrinsic RNA cleavage. We found that alkaline pH stimulated H1085Y to a much greater extent than WT, consistent with the metal cofactor results shown above. This result suggests that the cleavage activity is distinct from the activity observed in WT RNAP II. The pH profile for cleavage by WT (**Fig. 2E**, **Fig. S2**) shows little activity at pH 7–8 with the stimulation of hydrolysis starting around pH 8.5, and peaking at pH > 10. Alkaline pH stimulated cleavage by the H1085Y mutant enzyme to a much greater extent than for WT RNAP II (**Fig. 2E**, **Fig. S2**), increasing up to pH 9.5–10, which is in the neighborhood of the pK_a value for a tyrosine hydroxyl proton (9.6). This result is consistent with a contribution of an additional pH-sensitive group to cleavage in H1085Y that is not present in WT RNAP II. The tyrosine substitution effect was specific to H1085Y RNAP II, because when a tyrosine substitution mutant in the adjacent F1086 position was examined, it did not exhibit stimulation of intrinsic cleavage by pH beyond that for WT RNAP II.

TFIIS-stimulated cleavage is not affected by H1085Y

Factor-mediated cleavage of RNA 3′-ends by msRNAPs is independent of the TL, as the TL is displaced by cleavage factors that themselves contribute residues to msRNAP active sites to promote cleavage. It is possible that H1085Y intrinsic cleavage activity arises simply by increasing the fraction of complexes in an intrinsic cleavage-competent state, *i.e.* promoting backtracking, which might also result in increased sensitivity to factor-mediated

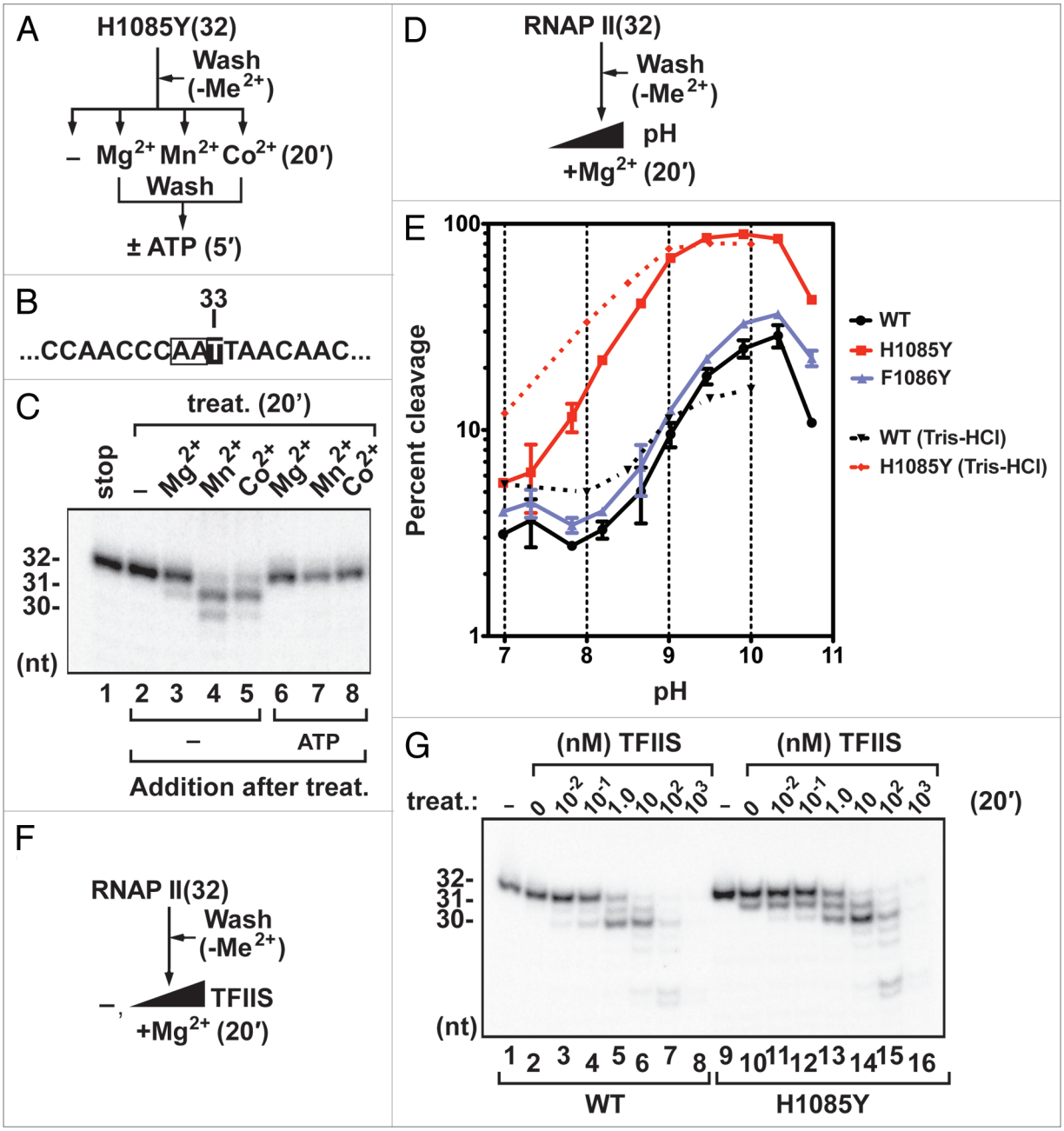

Figure 2. Characteristics of the intrinsic RNA cleavage mediated by H1085Y RNAP II. Starting with RNAP II elongation complexes stalled at +32 ("EC32," as in **Fig. 1**), a schematic outline next to each experiment indicates, in minutes, the order of additions and washes (without metals) for that panel. (**A**) Requirement for divalent metal cofactors and the ability of H1085Y active center to resynthesize the excised RNA. H1085Y(EC32) was incubated in the absence or presence of catalytic divalent cations. "-Me^{2+}" in the schematic indicates the absence of divalent metal cations in the wash buffer prior to readdition of divalent cations in each experiment as specified, followed by equilibration in buffer containing $MgCl_2$ with or without ATP for RNA re-synthesis. (**B**) Nucleotide sequence of the intrinsic cleavage template with the transcription stop highlighted (T33) and expected cleavage positions noted (A31, A30). (**C**) Determination of divalent cation preference for RNA cleavage (*lanes 3–5*) shows Mn^{2+} as the most potent cofactor at physiological pH (8.0). Re-synthesis of a 32-mer RNA with ATP only (*lanes 6–8*) indicates that 1- or 2- nt residues were excised (*lane 4 vs. 7, panel* **B**). (**D**) Dependence on alkaline pH. WT(EC32), H1085Y(EC32) and F1086Y(EC32) ECs were exposed to the basic range of the pH scale, from neutral (~7.0) to alkaline (~11), and intrinsic cleavage was quantified in (**E**), which shows a direct correlation between the efficiency of H1085Y-mediated cleavage and increasing pH (representative raw data shown in **Fig. S2**). Percent cleavage was determined by the amount of 31 nt RNA divided by the sum of 31/32 nt RNA. Note logarithmic scale for percent cleavage vs. pH. Error bars represent the range of two independent determinations or the standard deviation of three independent determinations. (**F**) TFIIS-supported hydrolysis of the second phosphodiester bond (P2) occurs concurrently and independently with the intrinsic cleavage of P1 with Mg^{2+}. Outlined in **F**, the experiment in gel panel (**G**) shows a dose-dependent appearance of a 2 nt-shortened RNA at 10–100 nM TFIIS for WT and H1085Y, while the 1-nt shortened RNA derived from H1085Y ECs still persists at these TFIIS concentrations (*lanes 13 and 14*). Experiments are representative of at least two independent determinations.

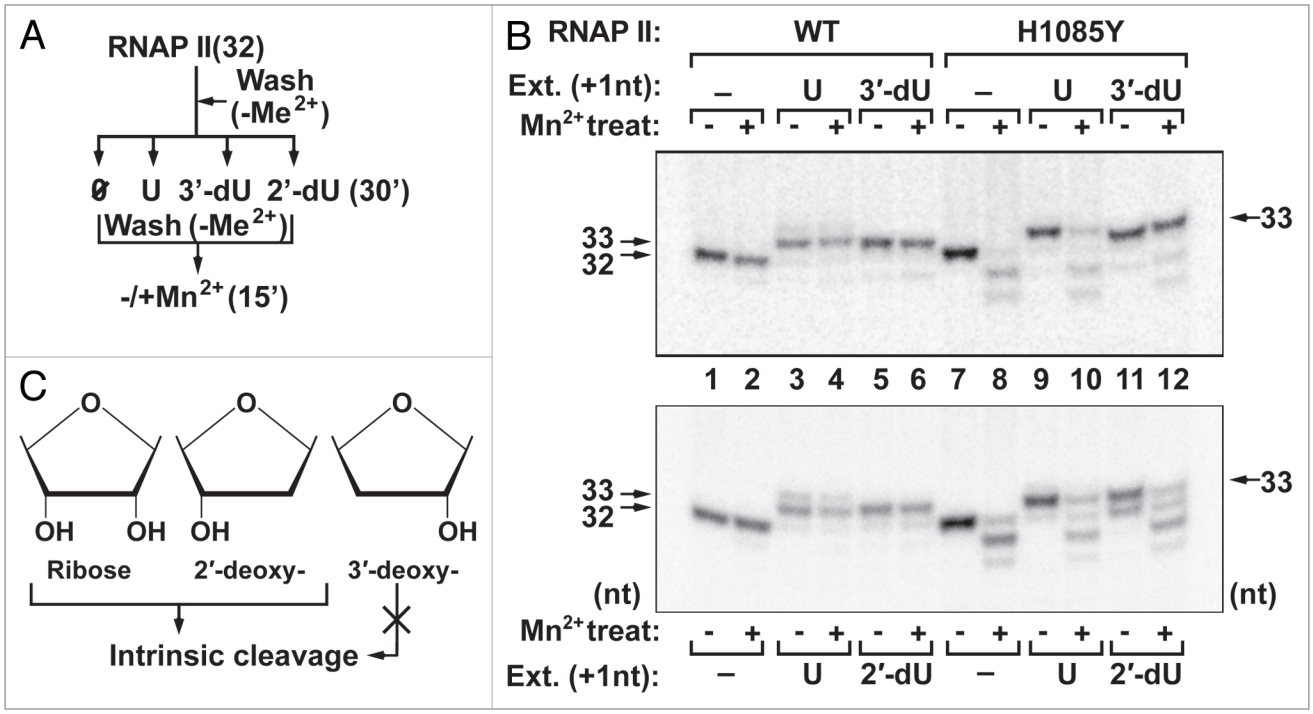

Figure 3. An intact 3′-hydroxyl group on the ribose of a 3′-terminal UMP is essential for H1085Y-mediated intrinsic cleavage. (**A**) As outlined, RNAP II EC32 (elongation complex with 32-mer RNA) complexes were divided and their nascent RNAs were extended by 1 nt with either UTP, 3′-deoxy-UTP or 2′-deoxy-UTP. Washes omitting metal cofactors are delineated as "-Me^{2+}." Following a washing step in the absence of metal cofactors, ECs were then exposed to Mn^{2+} ions to initiate intrinsic cleavage where appropriate. (**B**) Comparison of cleavage reactions by WT (RNA lengths; 32, 33 nt) and H1085Y (RNA lengths; 32, 33 nt) RNAP II enzymes. A terminal 3′-dUMP prevented RNA hydrolysis by H1085Y RNAP II (*lane 12*), while the WT RNAP II control lanes reveal little WT RNAP II cleavage activity regardless of the nature of the 3′-NMP added. (**C**) Structures of the tested 3′-NMP modified sugars are depicted. Experiments are representative of at least two independent determinations.

RNA cleavage. We therefore examined the sensitivities of WT and H1085Y stalled elongation complexes to TFIIS-mediated RNA cleavage. Direct comparison of intrinsic and TFIIS-supported cleavage (**Fig. 2F-G**) illustrates the TFIIS-dependent dinucleotide cleavage of 1-bp backtracked complexes (cleavage of the second phosphodiester bond), as reported previously (lanes 5 and 6).[40,41] Both the intrinsic and TFIIS-mediated cleavage reactions appear to occur in parallel for H1085Y, suggesting that H1085Y can enter the TFIIS cleavage-sensitive state with an efficiency similar to WT RNAP II. These results suggest that WT complexes stalled at this position are not generally defective for reverse translocation, which would be required for intrinsic cleavage of the first phosphodiester bond, as they can further reverse translocate to allow TFIIS-mediated cleavage of the second phosphodiester bond. The single-nucleotide shortened product of intrinsic cleavage also exhibits resistance to subsequent TFIIS-mediated hydrolysis (**Fig. 2G**, compare lanes 12, 13), indicating possible stabilization of this complex to further backtracking required for subsequent dinucleotide cleavage by TFIIS.

The 3′ hydroxyl group of the terminal NMP ribose moiety is essential for intrinsic cleavage of 3′-UMP by H1085Y

The natures of additional functional groups that might contribute to H1085Y's intrinsic cleavage are unknown. The involvement of the RNA 3′-OH in hydrolysis (transcript-assisted hydrolysis) has been studied through analyses of modified base and ribose moieties on the RNA 3′-NMP for a bacterial RNAP.[26,27] This reaction was found to require H1242 in *Taq* RNAP (analogous to *Sce* Rpb1 H1085). We focused on roles for the sugar moiety in the observed cleavage of H1085Y by incorporating modified NMPs at the 3′ terminal position of nascent RNA in elongation complexes. Elongation complexes containing nascent transcripts (33-mers) with a terminal UMP, 2′-deoxy-UMP or 3′-deoxy-UMP were treated with Mn^{2+} (**Fig. 3**). As expected, control WT elongation complexes remained relatively inert to Mn^{2+} challenge, regardless of the nature of the 3′-NMP (lanes 2,4,6). Consistent with the AMP-terminated 32-mers, a UMP at +33 allowed efficient cleavage by H1085Y RNAP II (see lanes 8 and 10 in both panels). However, a UMP analog lacking a 3′-hydroxyl failed to support intrinsic cleavage (upper panel, lane 12). 2′-deoxy-UTP-assisted hydrolysis (lower panel, lane 12) proceeded at a level comparable to UMP, and thus excludes a requirement for the 2′ hydroxyl in the reaction. Though requirements for the H1085Y-mediated RNAP II intrinsic cleavage are fundamentally different from the *Taq* β′ H1242-mediated intrinsic cleavage (requiring a distinct TL residue at the analogous TL position), for at least one cleavage product examined here, a similar requirement for a 3′-OH is observed. Contribution of the 3′-NMP to P2 cleavage in RNAP II complexes with mismatched 3′-ends has also been observed recently.[42]

H1085Y ECs remain sensitive to pyrophosphorolysis

Pyrophosphorolysis was used to determine whether stalled complexes were primarily pre-translocated (**Fig. 4A and B**).

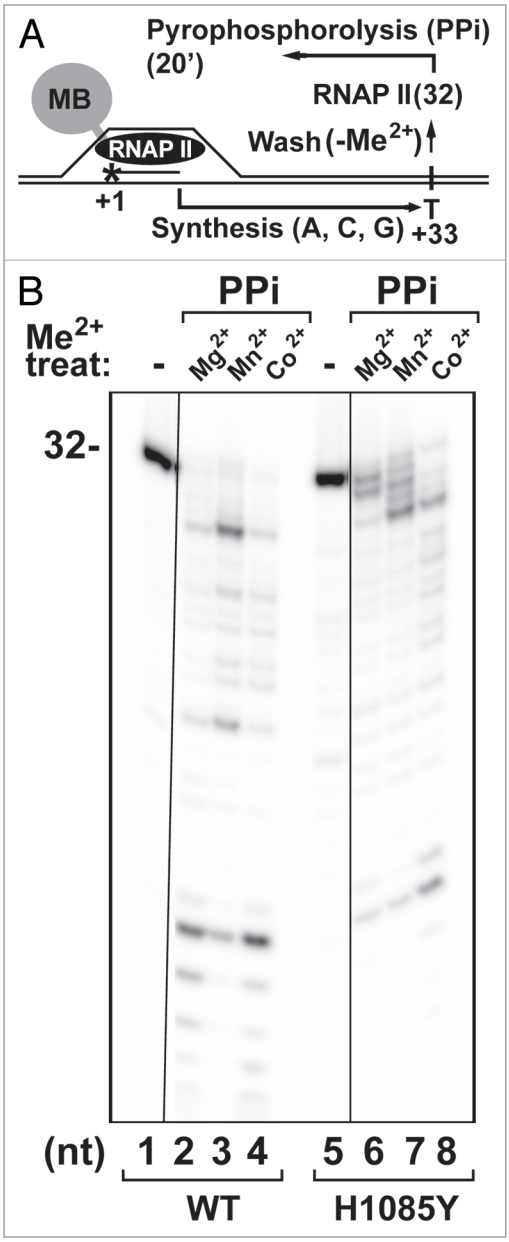

Figure 4. H1085Y RNAP II ECs retain sensitivity to pyrophosphorolysis. (**A**) Set-up for pyrophosphorolysis of nascent RNA in RNAP II EC32 complexes in the presence of different divalent cations. Washes omitting metal cofactors are delineated as "-Me^{2+}." (**B**) "Me^{2+} treat" indicates RNAP II EC treatment for pyrophosphorolysis in the presence of specified divalent metal (Me^{2+}) cations. Both WT and H1085Y RNAP II ECs are sensitive to pyrophosphorolysis, albeit H1085Y RNAP II shows lowered efficiency. Experiments are representative of at least two independent determinations.

Efficient pyrophosphorolysis would indicate efficient entry into the pre-translocated state, as this is the translocation state sensitive to pyrophosphorolysis. Conversely, resistance to pyrophosphorolysis would suggest possible stabilization of ECs in the post-translocated state. Both WT- (**Fig. 4B**, lanes 2–4) and H1085Y-synthesized RNAs (**Fig. 4B**, lanes 6–8) were sensitive to pyrophosphorolysis in the presence of Mg^{2+}, Mn^{2+}, or Co^{2+}, although H1085Y exhibited a lower efficiency of RNA degradation than WT, as expected from H1085Y defects in the converse reaction, RNA synthesis. Based on sensitivity to pyrophosphorolysis, the properties of the hydrolytic reactions by H1085Y are in agreement with those typical for pre-translocated and backtracked elongation complexes,[6] yielding the P1 and P2 bond cleavage, respectively. However, a step-wise exonuclease cleavage mechanism (P1 followed by P2) is an alternative possibility.

Mn^{2+} ions stimulate the H1085Y catalytic center for all transcription reactions

The findings illustrated in **Figure 4B** raised the possibility that Mn^{2+} could alleviate the H1085Y deficiency in nucleotidyl transfer (the reverse reaction to pyrophosphorolysis). To this end, WT and mutant RNAP II were assembled on a pre-opened template and tested for RNA synthesis in different stages of the transcription cycle using different catalytic metals. Mn^{2+} greatly stimulated abortive initiation by H1085Y (**Fig. 5B**, upper panels) as measured by generation of a 3-mer RNA product (**Fig. 5B**, lanes 19–22). Similarly, Mn^{2+}-catalyzed productive initiation (12-mer) by H1085Y (**Fig. 5B**, lower panels) was activated to near WT levels, as shown by the comparison of time points at 2 and 5 min (quantified in **Fig. S3**). It is of interest that Co^{2+}, which efficiently supported both of the degradative reactions, intrinsic cleavage (**Fig. 2C**) and pyrophosphorolysis (**Fig. 4B**), failed to efficiently support the forward reactions in either assay. Independent of RNAP II origin, multiple abortive signals were observed for Co^{2+} in single-round reactions for productive initiation (**Fig. 5B**, lower panels). Mn^{2+} stimulated H1085Y RNAP II elongation over a template enabling generation of a 358-nt run-off transcript, which is consistent with Mn^{2+} effects on H1085Y RNAP II in abortive and productive initiation assays generating short RNA products (**Fig. 6**, quantification in **Fig. S4**). In the elongation assay, H1085Y RNAP II treated with Mn^{2+} exhibited a similar or greater *average* elongation rate than WT with either Mg^{2+} or Mn^{2+}. The shapes of the run-off product accumulation curves, however, suggest that WT RNAP II reactions may have a greater contribution of both more quickly and more slowly elongating Polymerases to the measured rates than H1085Y. We speculate that a greater proportion of WT RNAP II enzymes pausing along the template is able to escape the pause(s) and contribute to run-off product than for H1085Y RNAP II, causing H1085Y RNAP II runoff production to appear more uniform.

Mn^{2+} and TFIIB compensate for H1085Y defects in responding to the stimulatory effect of TFIIF on the NAC

In order to probe possible cooperation of TFIIB or TFIIF with the RNAP II TL, we used different metal cofactors in conjunction with the TL mutant H1085Y in the abortive initiation assay (**Fig. 7**). Specific and regulated RNAP II initiation in vivo requires the contribution of a number of general transcription factors (GTFs), with two, TFIIB and TFIIF, particularly implicated in communication with the RNAP II active site. Although TFIIB has been proposed to stimulate rearrangements of RNAP II active site that consequently increase the affinity for metal B and stimulate catalysis,[36] the nature or mechanism of collaboration of either of these factors with the TL has not been determined. TFIIF has long been known to stimulate the elongation rate of RNAP II in

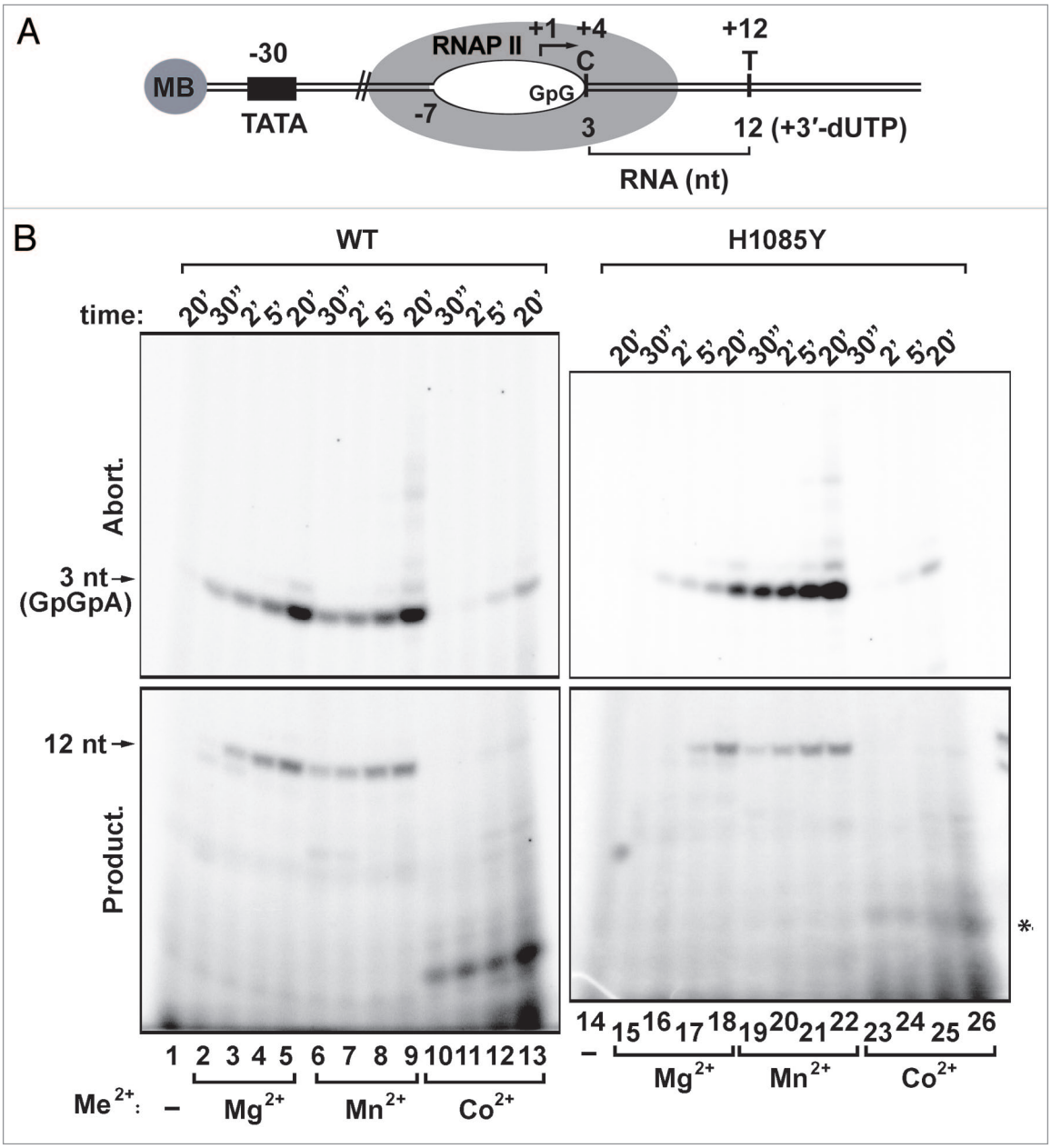

Figure 5. Mn^{2+} restores the catalytic activity of H1085Y RNAP II in both abortive and productive initiation. (**A**) Scheme of transcription initiation on a 5′-immobilized pre-melted template onto which RNAP II is assembled. Positions of the transcription bubble and sequence features (TATA box) are numbered relative to the designated TSS (+1). GpG-primed, [α-^{32}P]ATP-extended 3-mer or a 12-mer RNA generated with NTPs including [α-^{32}P] radiolabeled ATP, are indicated. (**B**) Effects of divalent cations on the formation of the second phosphodiester bond in GpGpA (abortive initiation) or synthesis of a 12-mer RNA (productive initiation) were measured over time courses. "Me^{2+}" indicates addition of divalent metal cations, which are specified under appropriate lanes of the gels shown. An asterisk marks abortive initiation products generated in productive initiation assays with Co^{2+} ions. Experiments are representative of at least two independent determinations.

vitro[43,44] while also showing functional interactions with TFIIB,[45] though recently, TFIIF regulation of RNAP II elongation per se has been reevaluated. However, in *S. cerevisiae* initiation, TFIIF has been reported to stimulate formation of the first two phosphodiester bonds on a pre-opened template and stabilize a short RNA-DNA hybrid in the active center.[46]

Assembled RNAP II-GTF-pre-melted template complexes, originating from equimolar combinations of GTFs and RNAP II's, produced a 3-mer RNA by incorporating radiolabeled ATP onto a dinucleotide primer over time (same assay as that in **Fig. 5B**). The calculated relative rates of abortive initiation (**Fig. 7B**), which were derived from the slope of linear regression lines (**Fig. S5**), recapitulate the published TFIIF stimulation of second phosphodiester formation by WT RNAP II[46] in the presence of Mg^{2+} (nearly 3-fold stimulation). We did not observe TFIIB stimulation of WT RNAP II abortive initiation in the

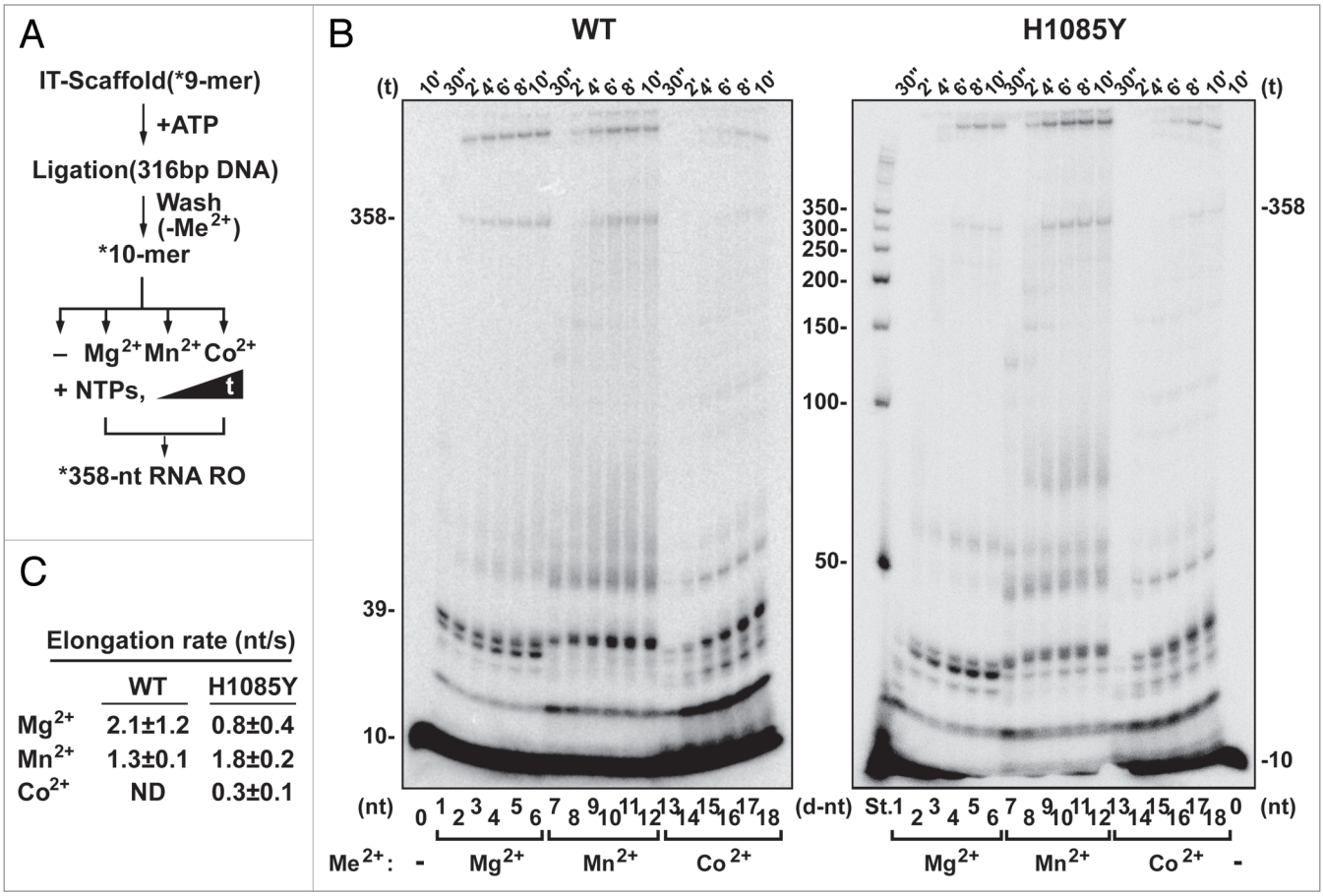

Figure 6. Mn^{2+} restores the elongation activity of H1085Y RNAP II. (**A**) Outline of the RNAP II elongation assay, based on the 5′-end template immobilized scaffold assembly (**Fig. 1A**) with a ligated DNA fragment at its 3′-end to extend the RNA Run-Off (RO) product to a final length of 358 nt. Wash omitting metal cofactors is delineated as "-Me^{2+}." "t" represents time course of NTP addition in the presence of specified divalent metal cations. (**B**) Time-dependent elongation of a 10-mer RNA in the presence of divalent cations. Non-advanced ECs (10-mer) and ECs, stopped due to a portion of the original scaffold complexes failing to ligate the long run-off template (39-mer), are indicated. ^{32}P-labeled DNA marker (*St.*) to approximate RNA transcript lengths is included. (**C**) Average elongation rates in nucleotides per second were derived from two to three independent experiments, plotted in **Figure S4**, where extension by 348 nts was used for calculations. Plus/minus values are the range of two determinations or the standard deviation of at least three determinations.

presence of Mg^{2+}, while H1085Y RNAP II was not stimulated either by TFIIB or TFIIF in the presence of Mg^{2+}. This result is striking because it suggests that TFIIF may function in a pathway that requires a WT TL. Alteration of the reaction parameters or functional geometry due to the presence of Mn^{2+} uncovered a small TFIIB effect on WT RNAP II but not H1085Y. Mn^{2+} also contributed to a robust stimulation of WT by TFIIF (5 to 6-fold stimulation), which was not significantly enhanced by TFIIB. TFIIB effects on WT RNAP II therefore appear additive at most with those of TFIIF in this abortive initiation assay. The presence of Mn^{2+} as metal cofactor uncovered the ability of TFIIF alone or in combination with TFIIB to stimulate transcription by H1085Y RNAP II. H1085Y was responsive to TFIIF (2-fold stimulation) and was further accelerated by TFIIB to a final 4-fold stimulation. These results suggest that TFIIB and TFIIF may cooperate to influence the Mn^{2+} -dependent active center within H1085Y RNAP II to stimulate catalysis. Taken together, they further suggest that TFIIF works with the TL under Mg^{2+}-dependent constraints on reaction function. The relaxation of reaction specificity through Mn^{2+} substitution for Mg^{2+} allowed TFIIB effects on the active site to be uncovered, and either bypasses a portion of the requirements for H1085 or allows greater contribution of Y1085 to abortive initiation.

H1085 substitution alters sensitivity of RNAP II activity to altered pH conditions

We determined how WT and H1085-substituted enzymes responded to altered pH for synthesis reactions (**Fig. 8**), as we had observed a number of pH effects on other active center reactions (**Fig. 2**). Structural identification of the TL as a substrate-interacting apparatus for RNAP II suggested a catalytic function for H1085 through donation of its proton to pyrophosphate.[7] Conservation of basic residues in analogous positions within the active sites of diverse and unrelated nucleic acid synthesis enzymes led to the proposal that these basic residues (and Rpb1 H1085 for *S. cerevisiae* RNAP II) function as general acids in phosphodiester bond formation reactions.[19] Studies with *Taq* RNAP did not show inhibition of the enzyme by alkaline conditions as would be necessary to assess function of *Taq* RNAP

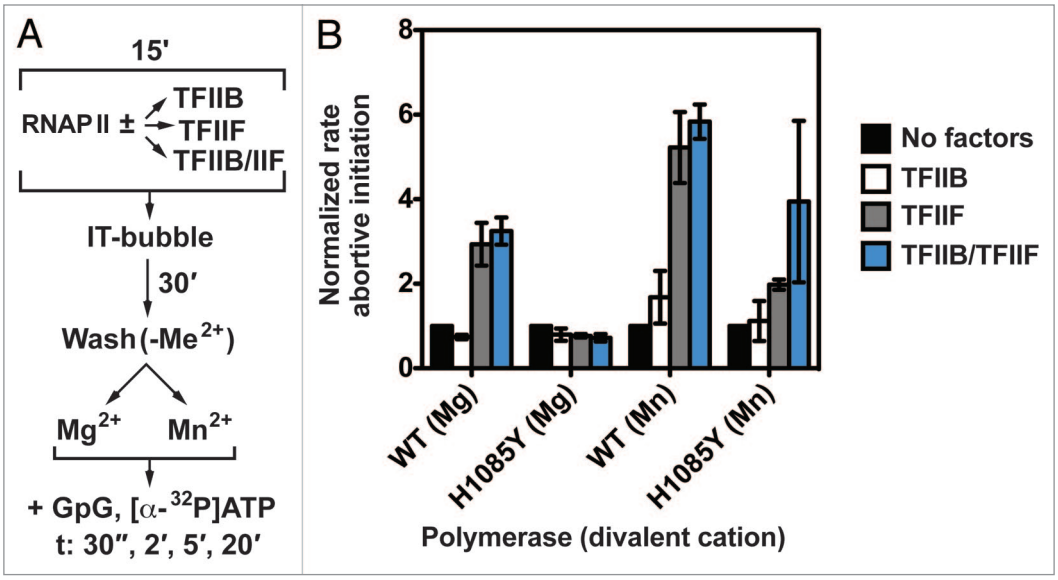

Figure 7. Mn^{2+} and TFIIB compensate for the deficiency of H1085Y in TFIIF stimulation of 3-mer RNA production. (**A**) The schematic timeline indicates, in minutes, the order of additions/washes for the experiment shown in **B**. WT and H1085Y RNAP II enzymes were preincubated with equimolar TFIIB or TFIIF, or TFIIB+TFIIF for 15 min at 25 °C. Following assembly on a bubble template, washed complexes were equilibrated in transcription buffer containing Mg^{2+} or Mn^{2+} ions and supplemented with a GpG dinucleotide primer and [α-^{32}P]ATP to initiate reactions for time points of 30 s and 2, 5, and 20 min. GpGpA products were quantified (**Fig. S5**) and the slope of linear regression lines calculated using GraphPad Prism 5.0d software. Wash omitting metal cofactors is delineated as "-Me^{2+}." (**B**) Plots represent the average relative rates of abortive initiation derived from linear regression with error bars indicating the range of two independent determinations, or the standard deviation of at least three determinations [No factors (black bars), TFIIB (white bars), TFIIF (gray bars), and TFIIB+TFIIF (blue bars)].

H1242 as a general acid.[17] We observed that WT RNAP II was strikingly inhibited by alkaline pH for both abortive (**Fig. 8**, **Fig. S6B-C**) and productive initiation (**Fig. S6C**). Mildly acidic treatment had little (abortive initiation, **Fig. 8B**) or a mild stimulatory effect (productive initiation, **Fig. S6C**). pH treatment had distinct effects on H1085Y abortive (**Fig. 8B**) or productive (**Fig. S6C**) initiation. First, H1085Y exhibited sensitivity to acidic conditions for both reactions. Second, H1085Y RNAP II showed partial resistance to alkaline conditions relative to WT RNAP II for abortive initiation, while showing complete resistance or slight stimulation by pH 9.5 for productive initiation. H1085Y effects may relate to the loss of H1085 instead of the gain of Y1085 (as observed for intrinsic cleavage). The relationships between ionizable groups in the TL (such as H1085 or Y1085) and the critical deprotonation of the RNA 3′-OH remain to be elucidated.

We utilized an additional H1085-substituted mutant enzyme, H1085Q, to assess function of H1085 in possible acid-base catalysis. While tyrosine is ionizable and can function in acid-base catalysis, glutamine is not. H1085Q, though less than H1085Y, confers some sensitivity to acidic conditions for RNAP II abortive (**Fig. 8B**) or productive initiation (**Fig. S6C**), suggesting that this feature partially relates to a loss of H1085 function (or gain of an H1085-inhibited function conferring acid sensitivity in the absence of H1085). Alkaline treatment reveals distinctions between H1085Y and H1085Q. For abortive initiation, H1085Q is more sensitive to alkaline treatment than H1085Y, but less so than WT. Results for both H1085 mutants are broadly consistent with H1085 functioning in acid-base catalysis. However, because tyrosine is ionizable, alkaline conditions may activate the H1085Y-substituted enzyme for synthesis at higher pH (see Discussion). Other distinctions between abortive initiation and productive initiation by H1085Y and H1085Q enzymes may relate to a number of factors. First, abortive initiation is a multi-round phenomenon and entails a substrate turnover step. Second, abortive initiation may be sensitive to positioning of the dinucleotide primer in ways that most of the NMP incorporations into a 12-mer might not be subject.

Surprisingly, the altered biochemical activity of H1085Y relative to WT RNAP II enzymes upon pH treatment or alteration of metal cofactor was reflected in the sensitivity or resistance of these enzymes to in vivo treatments (**Fig. 9**). A strain WT for *RPO21/RPB1* is sensitive to treatment with $MnCl_2$, with an *rpb1-E1103G* strain being markedly sensitive (**Fig. 9A**). In strong contrast to these strains, *rpb1-H1085Y* was not only resistant to $MnCl_2$, but in fact $MnCl_2$ treatment slightly suppressed *rpb1-H1085Y* growth defects (apparent at 10 mM $MnCl_2$). $MnCl_2$ sensitivity correlated with in vitro activity of RNAP II mutants (alleles for the most active RNAP II enzymes were the most sensitive in vivo) and showed the greatest allele-specificity in sensitivity, in contrast to the sensitivities observed for other metals (Fe, Zn, Cd, Liangtao Li and Jerry Kaplan, personal communication). $MnCl_2$ treatment may affect a Mg^{2+}-dependent process (e.g., the RNAP II active site), as supplementation of $MnCl_2$-treated media with $MgCl_2$ reversed the observed $MnCl_2$ effects. $MgCl_2$ alone had no observable effects on strain growth at the concentrations assayed (**Fig. 9A**).

Mildly altering the pH of growth medium by either alkaline treatment (10 mM NaOH) or acid treatment (10 mM HCl) also revealed allele-specific effects on RNAP II TL mutant strain

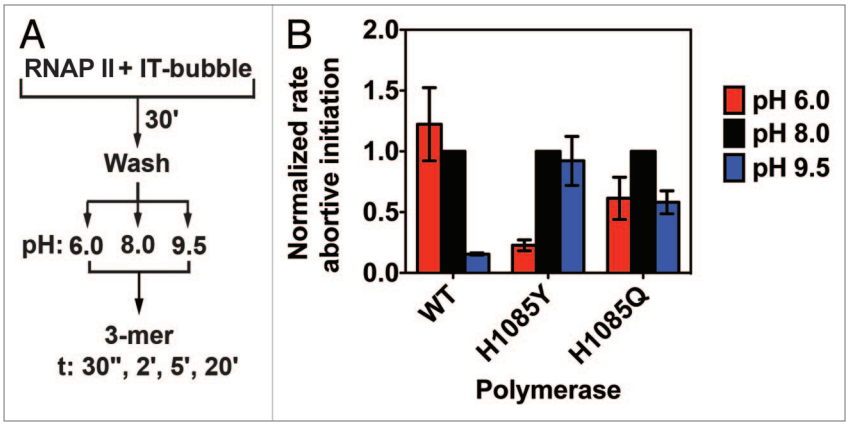

Figure 8. Trigger loop tyrosine at Rpo21/Rpb1 position 1085 is a candidate for acid-base catalysis during nucleotidyl transfer at alkaline pH. (**A**) RNAP II enzymes assembled on a IT-bubble nucleic acid scaffold were equilibrated in transcription buffer with pH 6.0, 8.0 and 9.5. Production of 3-mer RNAs by abortive initiation (3-mer) was monitored for 30 s, 2, 5, and 20 min time points. Average values from two to three experiments were plotted with the value for reaction at pH 8.0 set to 1 for each enzyme tested. A parallel experimental approach was always employed for comparison of transcription at pH 8.0 vs. 6.0 and for pH 8.0 vs. 9.5 for each enzyme. (**B**) In abortive initiation, H1085Y showed sensitivity to pH 6.0 and resistance to pH 9.5, while WT was resistant to pH 6.0 and sensitive to pH 9.5. H1085Q was partially sensitive to pH 6.0 and partially resistant to pH 9.5, relative to WT. Data are average of 2–3 independent replicates with error bars representing standard deviation (for three-replicate sets) or the range (for two-replicate sets).

growth (**Fig. 9B**). Generally, H1085 TL alleles were either resistant to the growth inhibition by NaOH exhibited by an *RPO21* RNAP II WT strain, or very slightly but reproducibly suppressed for growth defects. pH effects on RNAP II TL alleles by NaOH treatment were reversed by buffering the medium with equimolar HCl. These in vivo results are similar to the inhibition of WT RNAP II, and the resistance of H1085Y and H1085Q, to alkaline conditions in vitro.

Discussion

msRNAPs have highly conserved active sites throughout the kingdoms of life. Over evolutionary time, there has been divergence in their regulation by different constellations of factors in different species. As more is understood about mechanisms that control msRNAP active centers, increasing amounts of diversity in active center activities have been described.[28,47] The TL is the highly conserved focus of kinetic substrate selection and catalysis by msRNAPs, and contributes to pausing and translocation. While some residues are almost universally conserved, their contributions to different active center activities can be distinct in different species. For example, conserved substrate interacting residues differentially contribute to catalysis depending on species, with mutants showing a few fold effects in *E. coli* RNAP to ~100-fold effects for the analogous *T. aquaticus* RNAP mutants.[8,17] Differences in functions of conserved residues are even more apparent when examining intrinsic cleavage, and are discussed below.

Robust, efficient intrinsic cleavage has been observed for *Taq* RNAP, with *Eco* RNAP somewhat less efficient. The *Taq* intrinsic cleavage activity has different chemical group requirements depending on the nature of the 3′-NMP present in the RNA.[26] However, cleavage is highly if not completely dependent on *Taq* β′ H1242 (the residue analogous to Rpb1 H1085).[27] The cleavage observed in these cases is usually 2-nt from the 3′ end of the RNA. In contrast, *S. cerevisiae* RNAP II exhibits only very weak intrinsic cleavage. Here we demonstrate that a mutant variant of H1085, H1085Y, gains an intrinsic cleavage activity, presumably through alkaline activation by deprotonation of the tyrosyl hydroxyl. The activity observed for H1085Y with the RNA substrates tested here cleaves a single 3′-NMP, and is distinct from previously described msRNAP intrinsic cleavage activities. The function of the substituted tyrosine may be analogous to a tyrosine in the 3′-5′ exonuclease (exo) site of DNA RNAP I, which is proposed to orient an attacking hydroxyl through function as a general acid.[31,48] Analogy to the DNA RNAP I exo reaction has been noted for *Eco* RNAP cleavage of a single NMP,[28] yet H1085Y RNAP II has an even greater similarity in that a tyrosine residue heavily supports the reaction. The deprotonated Y1085 might also function as a general base to activate a water molecule for hydrolysis. Proximity of TL residues to the transcript 3′-end likely leads to a number of alternative conformations with any number of roles. The H1085Y gain of function we observe here for intrinsic cleavage also raises the possibilities of cryptic activities for other TL residues or substitutions therein.

It is generally accepted that msRNAPs utilize the universal two metal mechanism found in nucleic acid Polymerases to catalyze phosphodiester bond formation,[49,50] but the role of a conserved basic residue within the TL, Rpb1 H1085 and its analogs in other msRNAPs, is not defined. This histidine has been proposed as a proton donor for acid-base catalysis, yet evidence from other msRNAPs for this has been difficult to obtain. This question has been most closely addressed in the *T. aquaticus* system, however *Taq* RNAP does not exhibit a descending limb of reduced activity upon increasing pH, so any effects of removing proton donation by its TL β′ H1242 would be obscured. It is also likely that this histidine has roles in addition to proton donation. Residues substituted for H1085 in yeast that are less likely (tyrosine) or very unlikely (arginine) to donate a proton at physiological pH, or unable to donate (glutamine or tryptophan), are all able to support viability, while an alanine substitution does not. These results suggest functions for side chains at this position beyond the ability to be ionized. Our studies here reveal that yeast RNAP II activity is inhibited at alkaline pH. Substitution of H1085 alters the behavior of the enzyme, showing resistance to alkaline treatment, which is consistent with H1085 functioning as a general acid for catalysis. Yeast RNAP II is therefore a good candidate for more sophisticated enzymology and proton inventory experiments to assess the role of H1085. In the two metal ion

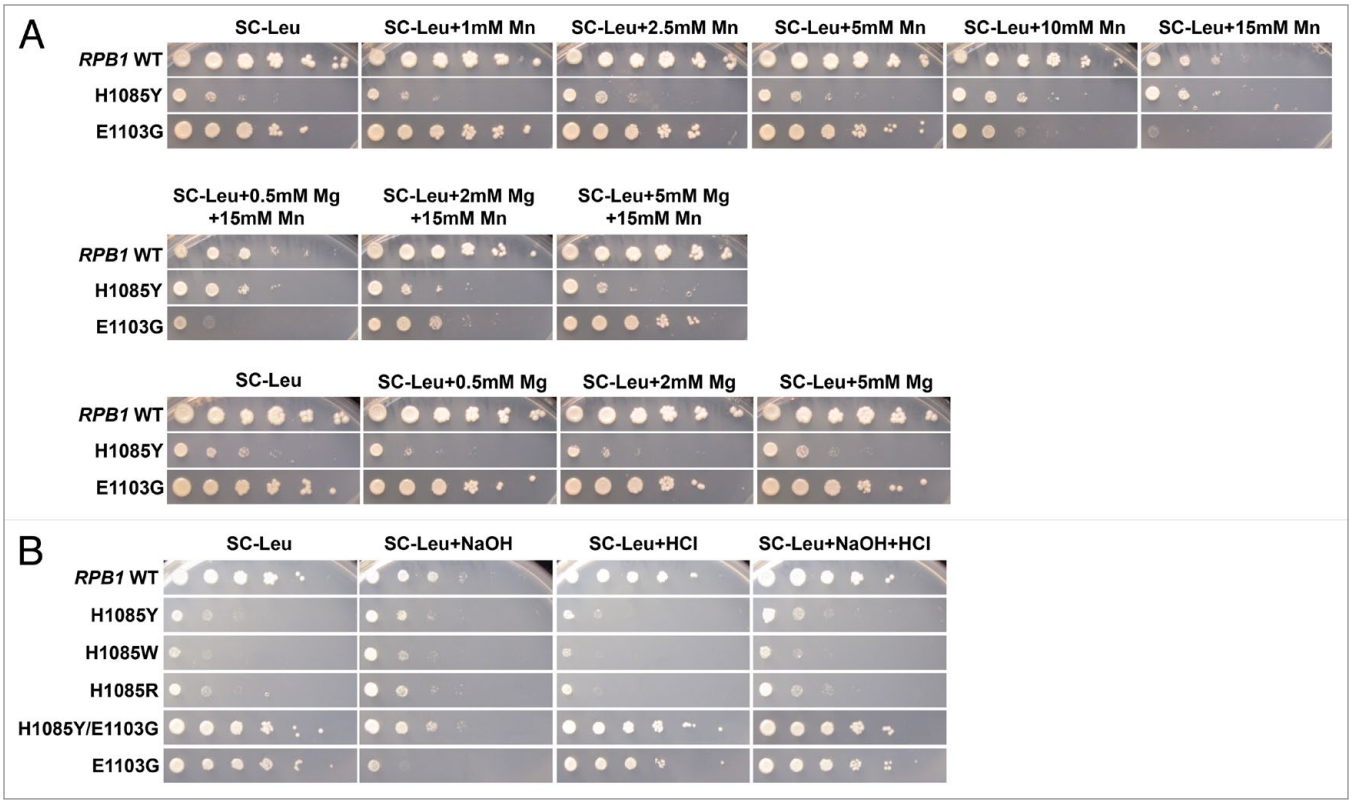

Figure 9. In vivo effects of Mn^{2+} treatment and alteration of media pH on RNAP II TL mutants. (**A**) 10-fold serial dilutions of *rpb1* TL WT, H1085Y and E1103G strains spotted onto media without or supplemented with increasing concentrations of $MnCl_2$ or $MnCl_2$ supplemented with $MgCl_2$. (**B**) Mild pH treatment on growth plates was accomplished by supplementation of standard media with 10 mM NaOH or 10 mM HCl or both. 10-fold serial dilutions of *rpo21/rpb1* TL mutants and a control *RPO21/RPB1* WT strain are shown.

mechanism for phosphodiester bond formation, metal A(I) Mg^{2+} is proposed to lower the pK_a of the 3′-hydroxyl of the terminal NMP, allowing deprotonation at physiological pH. We speculate an analogous role for Mn^{2+} A(I), or generally both Mn^{2+} ions, in lowering the pK_a of the Y1085 side chain hydroxyl at 'transcription/cleavage physiological' pH 8, facilitating deprotonation. The proton would subsequently be donated to the β-phosphate oxygen during catalysis. In intrinsic cleavage, proton donation (general acid), proton receiving (general base), or direct involvement of tyrosyl O^- as a nucleophile are all possible and are difficult to distinguish because of likely contribution of multiple pH-sensitive groups to the reaction. Further studies will identify the precise role of Y1085.

The next major questions in detailing RNAP II and msRNAP mechanisms relate to the functions of regulatory factors and an understanding at the atomic level how they might impinge on the active center. Indeed, a number of structures of msRNAP enzymes with additional factors describe their positions in the enzyme complexes (for review see ref. 9). It is not clear how factors might communicate or collaborate with the active center to alter transcription. Recent work has implicated TFIIB, an essential RNAP II GTF, as an allosteric effector of the RNAP II active site.[36] TFIIB, in cooperation with TBP, has been shown to stimulate transcription initiation from premelted DNA template,[51,52] suggesting functions beyond open complex formation. In work here, we present evidence that TFIIB alters active center function. These effects were uncovered through the use of a TL mutant and substitution of Mn^{2+} for Mg^{2+} as the metal cofactor.

Intriguingly, we find that TFIIF requires a WT TL to stimulate transcription in an abortive transcription assay. As mentioned above, TFIIF has long been known to stimulate RNAP II elongation rate in vitro,[43,44] though the in vivo relevance of this activity during elongation is less clear.[53,54] In studies utilizing a preformed transcription bubble template with RNAP II, TFIIB and TBP, TFIIF was strongly stimulatory.[55] TFIIF also stabilized TFIIB in initiation complexes.[45] Whether TFIIF stimulates catalysis or product turnover in abortive initiation is an open question and will be critical for understanding the relationship between TFIIF and the TL. While TFIIF was shown to stimulate early abortive RNA formation by RNAP II alone using a pre-melted template, it also stabilized RNA 5-mer association with RNAP II.[46] Such stabilization effects on 2-mer primer association or 3-mer product have not been determined and could be stimulatory for a 2-mer if 2-mer association were limiting, but possibly inhibitory for a 3-mer product if turnover became limiting. Differences in Mn^{2+} and TFIIF stimulation of abortive initiation suggest these treatments might be differentially altering steps in the abortive initiation assay. First, Mn^{2+} showed an increased ability to stimulate H1085Y over WT RNAP II. Second, Mn^{2+} stimulation resulted in a behavior of abortive initiation that appeared biphasic (**Fig.**

S3). An apparent burst phase can be detected at the first time point, which is consistent with simulation of catalysis early in the reaction, but with possibly limiting product turnover dominating later time points in the assay. This is in contrast to the behavior of TFIIF and of pH in the control of abortive initiation, which are well-described by linear fits (**Figs. S5** and **S6**). Second, TFIIF is unable to stimulate H1085Y in the presence of Mg^{2+}, but does stimulate WT RNAP II (**Fig. 7**). Our results suggest that TFIIF modulates a TL-sensitive step in the transcription process, but the exact step remains to be determined. If Mn^{2+} is presumed to primarily affect catalysis, distinctions between Mn^{2+} and TFIIF behavior may indicate that TFIIF functions elsewhere or has multiple roles.

In summary, we identify a new intrinsic RNA cleavage activity of the first phosphodiester bond that is acquired through substitution of histidine for tyrosine at trigger loop position 1085 in yeast Rpo21/Rpb1. Y1085 likely acts as a general acid for RNA hydrolysis and nucleotidyl transfer in an alkaline environment. Out of three catalytic metals, Mn^{2+} is the most efficient for RNA cleavage and synthesis, i.e., early phosphodiester bond formation, initiation and elongation by the H1085Y RNAP II per se. Furthermore, Mn^{2+} enables further TFIIB-TFIIF collaboration in reactivating the H1085Y RNAP II active site. In support of observed biochemical effects on RNAP II in vitro, Mn^{2+} and alkaline pH partially suppress H1085Y growth defects in vivo.

Materials and Methods

Reagents

rNTPs and 2′-deoxy-dATP were obtained from GE Healthcare Life Sciences; [α-^{32}P] ATP and [γ-^{32}P] ATP from Perkin-Elmer; 2′-deoxy-UTP, 3′-deoxy-UTP and dinucleotide GpG from TriLink Biotechnologies. RNase inhibitor, T4 Polynucleotide kinase, T4 DNA Ligase, and 50 bp DNA ladder were purchased from Fermentas/Thermo.

Protein preparations

Yeast RNAP II enzymes and cleavage factor TFIIS were purified as described previously.[7,15,56] *E. coli*-overexpressed, hexahistidine-tagged TFIIB was isolated via a chitin-binding followed by intein cleavage and an additional purification on TALON metal affinity resin (Clontech Laboratories) according to the manufacturer's instructions (as described by Liu et al.[57]). TFIIF was kindly provided by Kenji Murakami.

Assembly of elongation complexes, advance to the downstream T33 stop and treatment of stalled complexes

Procedure for the immobilized scaffold formation was based on and modified from method devised by Kashlev group.[58] Typically, 10 μl reactions contained 1.25 pmol of template oligonucleotide TS69, 2.5 pmol 5′-end ^{32}P-labeled 9-mer RNA (RNA9), 0.5 μg RNAP II and 1.25 pmol of the fully complementary nontemplate 5′-biotinylated NTS69 in Transcription Buffer (TB) (20 mM TRIS-HCl, pH 8.0, 40 mM KCl, 5 mM $MgCl_2$ and 1 mM DTT) (TB40 for 40 mM KCl, TB1000 for 1000 mM KCl, etc.). TS69: 5′-CCGGA CCCCG GTGTT AATTG GGTTG GCTTT TCGCC GCGCT CCTCT CGATG GCTGT AAGTA TTCTA GAGG-3′. RNA9: 5′-AUCGAGAGG-3′. Scaffold templates were attached on streptavidin-coupled Dynabeads M-280 (Invitrogen). ECs were washed twice with low salt TB40/0.1%NP40 buffers (TB containing 10% glycerol, 0.25 mg/ml BSA) and equilibrated in TB40 without NP40. In some experiments NP40 was reduced to 0.02%. This washing protocol was used after each experimental step with immobilized ternary complexes. ECs were then walked to T33 stop with 0.2 mM of each of ATP, CTP, GTP in the presence of RNase inhibitor (0.4U/μl) at 25 °C for 5 min. Stalled complexes were washed with buffers without $MgCl_2$. Transcripts in **Figure 3** were extended by 1 nt with 0.5 mM of UTP or deoxy-UTP derivative in TB40 and washed again in the absence of metal. As indicated in individual experiments, ECs were subjected to the treatment with 5 mM of divalent metal (2 mM $MnCl_2$ in **Figure 4B**), 2 mM Na-Pyrophoshate, range of pH, and increasing concentrations of TFIIS or metals in **Figures 2G** and **S1**, respectively. In pyrophosphorolysis and TFIIS cleavage experiments, ECs were treated with an additional wash in TB1000/0.1%NP40 for 10 min preceding low salt washes before and after EC32 formation. For pH treatment, complexes were washed as above for assembly and transcription and then equilibrated in TB40 (no Mg^{2+}) but with Tris buffer replaced by a combination buffer of 25 mM each MOPS, CHES, CAPS, TAPS (Sigma-Aldrich) adjusted to desired pH. In **Figure 2C**, the washed metal-treated complexes were supplemented with 0.2 mM ATP. RNAs were resolved on 20% polyacrylamide/8 M urea gels. Gels were imaged with Bio-Rad Imager and quantified with ImageQuant software 5.2 (GE Healthcare).

Elongation assay

Scaffold assembly and immobilization on streptavidin-paramagnetic beads proceeded as described above with 5′-phosphorylated TS59 and 5′-biotinylated NTS62. TS59: 5′-GTGTT AATTG GGTTG GCTTT TCGCC GCGCT CCTCT CGATG GCTGT AAGTA TTCTA GAGG-3′, NTS62: 5′-CCTCT AGAAT ACTTA CAGCC ATCGA GAGGA GCGCG GCGAA AAGCC AACCC AATTA ACACG GG-3′. These complementary oligonucleotides created the DraIII 3′ end overhang after annealing. Scaffold template was extended downstream by ligation to a long double stranded (ds) DNA fragment, PCR-amplified yeast TFIIB coding sequence with generated DraIII site at the 5′ end. 2.5 pmol of 316 bp DNA (cut with DraIII) was added to the reaction consisting of TB with 2% PEG 8000, 2 mM ATP and 200 U T4 DNA Ligase, followed by incubation at 12 °C for 1 h. Free DNA was washed off and purified ECs contained ^{32}P-labeled 10-mer RNA, because of sequence dependent addition of one A in the course of ligation. Prior and subsequent to ligation, ECs were washed as detailed in the section above, including high salt TB1000 washes followed by the specified low salt TB40 washes. Elongation was resumed with 0.5 mM of each NTP, 5 mM of relevant metal and RNase inhibitor included. RNA products were run on denaturating 6% polyacrylamide/8 M urea gels along with radiolabeled 50 bp DNA ladder and run-off fractions quantified.

Abortive and productive initiation

Pre-opened (from -7 to +3 relative to the transcription start site) template 83 was derived from bubble80 template.[46] TS83:

5′-TGAAG TCTTG TGTGG TCCTG AGAAA GTGTT GTGtc ctctg acaGA AAGAT TAATA ATTGT ATGAC TATTT ATACG CGTCC TGT-3′, NTS83: 5′-Biotin ACAGG ACGCG TATAA ATAGT CATAC AATTA TTAAT CTTTC acgat ctatt CACAA CACTT TCTCA GGACC ACACA AGACT TCA-3′. Annealed oligonucleotides were gel purified (2% agarose) and ds template attached on streptavidin-M280 beads via its 5′ biotinylated end. To assemble pre-initiation complexes (PICs), 0.91 pmol of RNAP II was added to 85 ng of immobilized template in TB50 for 30 min at 25 °C. When RNAP II and GTFs preincubations were required, equimolar amounts of RNAP II, TFIIB or/and TFIIF (0.91 pmol of each) were mixed for 15 min at 25 °C before addition to template. Transcriptionally competent complexes were purified with one TB100/NP-40 wash, followed by two washes with TB50/NP-40. All transcription reactions were performed in TB50, 5 mM of relevant metal and pH (TRIS-HCl) as indicated. Abortive initiation assays were run with 0.5 mM GpG and 0.5 μM [α-^{32}P] ATP. Productive transcriptions were initiated with 1 mM GpG, 50 μM ATP, 0.5 μM [α-^{32}P] ATP, 0.2 mM CTP and 0.1 mM 3′-deoxy-UTP as a chain terminator at the first downstream T stop. Both types of initiations contained RNase inhibitor. Transcripts were resolved on 28% (for trinucleotides) and 20% (for 12-mers) denaturing polyacrylamide gels and quantified as described above.

Yeast media and strains

Yeast strains used in in vivo growth assay with metals are derived from S288C,[59] 10-fold serial dilutions of saturated cultures of yeast strains were plated on different media for spot assays. RNAP II mutant plasmids are pRS315 *LEU2*-based,[60] transformed into CKY283 (*rpb1*Δ, described in refs. 9, 15) followed by plasmid shuffling with 5-fluoroorotic acid (5FOA, Gold Biotechnology) to select for loss of *RPB1 URA3* plasmid.[61] Yeast minimal media (synthetic complete, SC with amino acid drop out) are prepared in standard fashion as described in Amber et al.[62] with the following alterations: per standard batch formulation Adenine Hemisulfate (if added) was 2g, Uracil (if added) was 2g, myo-inositol was 0.1g, p-Aminobenzoic acid (PABA) was 0.2g. Manganese ($MnCl_2$, Sigma-Aldrich) and Magnesium ($MgCl_2$, VWR) were added from 1M stocks to final concentrations noted in **Figure 9**. Media with altered pH were prepared using 1 N stocks of NaOH and HCl solutions to generate final concentrations noted in **Figure 9**.

Funding

This work was supported by the Welch Foundation [grant number A-1763 to CDK]; and by the US National Institutes of Health National Institute of General Medical Sciences [grant number R01GM097260 to CDK]. The content is solely the responsibility of the authors and does not necessarily represent the official views of the funding agencies.

Disclosure of Potential Conflicts of Interest

No potential conflicts of interest were disclosed.

Acknowledgments

We thank Frank Raushel and Greg Reinhart for suggestions regarding pH analysis of intrinsic cleavage. We thank Kenji Murakami for the gift of TFIIF. We thank Jerry Kaplan, Feng Qiao, and members of the Kaplan lab for comments on the manuscript and Dave Peterson and Mary Bryk for advice.

Authors contributions: PČ: conception and design of studies, performed experiments, analysis and interpretation of data, and wrote the manuscript. HJ, LL: contributed experimental data on in vivo analysis of RNAP II mutants. CDK: performed subset of experiments, input on experimental design, analysis and interpretation, co-wrote manuscript with PČ.

Supplementary Material

Supplementary material may be found here:
https://www.landesbioscience.com/journals/transcription/article/28869/

References

1. Yuzenkova Y, Roghanian M, Zenkin N. Multiple active centers of multi-subunit RNA polymerases. Transcription 2012; 3:115-8; PMID:22771945; http://dx.doi.org/10.4161/trns.19887
2. Whitehall SK, Bardeleben C, Kassavetis GA. Hydrolytic cleavage of nascent RNA in RNA polymerase III ternary transcription complexes. J Biol Chem 1994; 269:2299-306; PMID:7507490
3. Tschochner H. A novel RNA polymerase I-dependent RNase activity that shortens nascent transcripts from the 3′ end. Proc Natl Acad Sci U S A 1996; 93:12914-9; PMID:8917519; http://dx.doi.org/10.1073/pnas.93.23.12914
4. Weilbaecher RG, Awrey DE, Edwards AM, Kane CM. Intrinsic transcript cleavage in yeast RNA polymerase II elongation complexes. J Biol Chem 2003; 278:24189-99; PMID:12692127; http://dx.doi.org/10.1074/jbc.M211197200
5. Rudd MD, Luse DS. Amanitin greatly reduces the rate of transcription by RNA polymerase II ternary complexes but fails to inhibit some transcript cleavage modes. J Biol Chem 1996; 271:21549-58; PMID:8702941; http://dx.doi.org/10.1074/jbc.271.35.21549
6. Orlova M, Newlands J, Das A, Goldfarb A, Borukhov S. Intrinsic transcript cleavage activity of RNA polymerase. Proc Natl Acad Sci U S A 1995; 92:4596-600; PMID:7538676; http://dx.doi.org/10.1073/pnas.92.10.4596
7. Wang D, Bushnell DA, Westover KD, Kaplan CD, Kornberg RD. Structural basis of transcription: role of the trigger loop in substrate specificity and catalysis. Cell 2006; 127:941-54; PMID:17129781; http://dx.doi.org/10.1016/j.cell.2006.11.023
8. Zhang J, Palangat M, Landick R. Role of the RNA polymerase trigger loop in catalysis and pausing. Nat Struct Mol Biol 2010; 17:99-104; PMID:19966797; http://dx.doi.org/10.1038/nsmb.1732
9. Kaplan CD, Jin H, Zhang IL, Belyanin A. Dissection of Pol II trigger loop function and Pol II activity-dependent control of start site selection in vivo. PLoS Genet 2012; 8:e1002627; PMID:22511879; http://dx.doi.org/10.1371/journal.pgen.1002627
10. Kaplan CD. Basic mechanisms of RNA polymerase II activity and alteration of gene expression in Saccharomyces cerevisiae. Biochim Biophys Acta 2013; 1829:39-54; PMID:23022618; http://dx.doi.org/10.1016/j.bbagrm.2012.09.007
11. Bar-Nahum G, Epshtein V, Ruckenstein AE, Rafikov R, Mustaev A, Nudler E. A ratchet mechanism of transcription elongation and its control. Cell 2005; 120:183-93; PMID:15680325; http://dx.doi.org/10.1016/j.cell.2004.11.045
12. Dangkulwanich M, Ishibashi T, Liu S, Kireeva ML, Lubkowska L, Kashlev M, Bustamante CJ. Complete dissection of transcription elongation reveals slow translocation of RNA polymerase II in a linear ratchet mechanism. Elife 2013; 2:e00971; PMID:24066225; http://dx.doi.org/10.7554/eLife.00971
13. Feig M, Burton ZF. RNA polymerase II with open and closed trigger loops: active site dynamics and nucleic acid translocation. Biophys J 2010; 99:2577-86; PMID:20959099; http://dx.doi.org/10.1016/j.bpj.2010.08.010
14. Larson MH, Zhou J, Kaplan CD, Palangat M, Kornberg RD, Landick R, Block SM. Trigger loop dynamics mediate the balance between the transcriptional fidelity and speed of RNA polymerase II. Proc Natl Acad Sci U S A 2012; 109:6555-60; PMID:22493230; http://dx.doi.org/10.1073/pnas.1200939109

15. Kaplan CD, Larsson KM, Kornberg RD. The RNA polymerase II trigger loop functions in substrate selection and is directly targeted by alpha-amanitin. Mol Cell 2008; 30:547-56; PMID:18538653; http://dx.doi.org/10.1016/j.molcel.2008.04.023
16. Kireeva ML, Nedialkov YA, Cremona GH, Purtov YA, Lubkowska L, Malagon F, Burton ZF, Strathern JN, Kashlev M. Transient reversal of RNA polymerase II active site closing controls fidelity of transcription elongation. Mol Cell 2008; 30:557-66; PMID:18538654; http://dx.doi.org/10.1016/j.molcel.2008.04.017
17. Yuzenkova Y, Bochkareva A, Tadigotla VR, Roghanian M, Zorov S, Severinov K, Zenkin N. Stepwise mechanism for transcription fidelity. BMC Biol 2010; 8:54; PMID:20459653; http://dx.doi.org/10.1186/1741-7007-8-54
18. Fouqueau T, Zeller ME, Cheung AC, Cramer P, Thomm M. The RNA polymerase trigger loop functions in all three phases of the transcription cycle. Nucleic Acids Res 2013; 41:7048-59; PMID:23737452; http://dx.doi.org/10.1093/nar/gkt433
19. Castro C, Smidansky ED, Arnold JJ, Maksimchuk KR, Moustafa I, Uchida A, Götte M, Konigsberg W, Cameron CE. Nucleic acid polymerases use a general acid for nucleotidyl transfer. Nat Struct Mol Biol 2009; 16:212-8; PMID:19151724; http://dx.doi.org/10.1038/nsmb.1540
20. Vassylyev DG, Vassylyeva MN, Zhang J, Palangat M, Artsimovitch I, Landick R. Structural basis for substrate loading in bacterial RNA polymerase. Nature 2007; 448:163-8; PMID:17581591; http://dx.doi.org/10.1038/nature05931
21. Carvalho ATP, Fernandes PA, Ramos MJ. The Catalytic Mechanism of RNA Polymerase II. J Chem Theory Comput 2011; 7:1177-88; http://dx.doi.org/10.1021/ct100579w
22. Shimamoto N. Nanobiology of RNA polymerase: biological consequence of inhomogeneity in reactant. Chem Rev 2013; 113:8400-22; PMID:24074222; http://dx.doi.org/10.1021/cr400006b
23. Wang B, Feig M, Cukier RI, Burton ZF. Computational simulation strategies for analysis of multisubunit RNA polymerases. Chem Rev 2013; 113:8546-66; PMID:23987500; http://dx.doi.org/10.1021/cr400046x
24. Seibold SA, Singh BN, Zhang C, Kireeva M, Domecq C, Bouchard A, Nazione AM, Feig M, Cukier RI, Coulombe B, et al. Conformational coupling, bridge helix dynamics and active site dehydration in catalysis by RNA polymerase. Biochim Biophys Acta 2010; 1799:575-87; PMID:20478425; http://dx.doi.org/10.1016/j.bbagrm.2010.05.002
25. Wang D, Bushnell DA, Huang X, Westover KD, Levitt M, Kornberg RD. Structural basis of transcription: backtracked RNA polymerase II at 3.4 angstrom resolution. Science 2009; 324:1203-6; PMID:19478184; http://dx.doi.org/10.1126/science.1168729
26. Zenkin N, Yuzenkova Y, Severinov K. Transcript-assisted transcriptional proofreading. Science 2006; 313:518-20; PMID:16873663; http://dx.doi.org/10.1126/science.1127422
27. Yuzenkova Y, Zenkin N. Central role of the RNA polymerase trigger loop in intrinsic RNA hydrolysis. Proc Natl Acad Sci U S A 2010; 107:10878-83; PMID:20534498; http://dx.doi.org/10.1073/pnas.0914424107
28. Sosunova E, Sosunov V, Epshtein V, Nikiforov V, Mustaev A. Control of transcriptional fidelity by active center tuning as derived from RNA polymerase endonuclease reaction. J Biol Chem 2013; 288:6688-703; PMID:23283976; http://dx.doi.org/10.1074/jbc.M112.424002
29. Brueckner F, Cramer P. Structural basis of transcription inhibition by alpha-amanitin and implications for RNA polymerase II translocation. Nat Struct Mol Biol 2008; 15:811-8; PMID:18552824; http://dx.doi.org/10.1038/nsmb.1458
30. Roghanian M, Yuzenkova Y, Zenkin N. Controlled interplay between trigger loop and Gre factor in the RNA polymerase active centre. Nucleic Acids Res 2011; 39:4352-9; PMID:21266474; http://dx.doi.org/10.1093/nar/gkq1359
31. Beese LS, Steitz TA. Structural basis for the 3′-5′ exonuclease activity of Escherichia coli DNA polymerase I: a two metal ion mechanism. EMBO J 1991; 10:25-33; PMID:1989886
32. Niyogi SK, Feldman RP. Effect of several metal ions on misincorporation during transcription. Nucleic Acids Res 1981; 9:2615-27; PMID:7024904; http://dx.doi.org/10.1093/nar/9.11.2615
33. Hoffman DJ, Niyogi SK. Metal mutagens and carcinogens affect RNA synthesis rates in a distinct manner. Science 1977; 198:513-4; PMID:910143; http://dx.doi.org/10.1126/science.910143
34. Liu X, Bushnell DA, Kornberg RD. RNA polymerase II transcription: structure and mechanism. Biochim Biophys Acta 2013; 1829:2-8; PMID:23000482; http://dx.doi.org/10.1016/j.bbagrm.2012.09.003
35. Grünberg S, Hahn S. Structural insights into transcription initiation by RNA polymerase II. Trends Biochem Sci 2013; 38:603-11; PMID:24120742; http://dx.doi.org/10.1016/j.tibs.2013.09.002
36. Sainsbury S, Niesser J, Cramer P. Structure and function of the initially transcribing RNA polymerase II-TFIIB complex. Nature 2013; 493:437-40; PMID:23151482; http://dx.doi.org/10.1038/nature11715
37. Braberg H, Jin H, Moehle EA, Chan YA, Wang S, Shales M, Benschop JJ, Morris JH, Qiu C, Hu F, et al. From structure to systems: high-resolution, quantitative genetic analysis of RNA polymerase II. Cell 2013; 154:775-88; PMID:23932120; http://dx.doi.org/10.1016/j.cell.2013.07.033
38. Malagon F, Kireeva ML, Shafer BK, Lubkowska L, Kashlev M, Strathern JN. Mutations in the Saccharomyces cerevisiae RPB1 gene conferring hypersensitivity to 6-azauracil. Genetics 2006; 172:2201-9; PMID:16510790; http://dx.doi.org/10.1534/genetics.105.052415
39. Imashimizu M, Kireeva ML, Lubkowska L, Gotte D, Parks AR, Strathern JN, Kashlev M. Intrinsic translocation barrier as an initial step in pausing by RNA polymerase II. J Mol Biol 2013; 425:697-712; PMID:23238253; http://dx.doi.org/10.1016/j.jmb.2012.12.002
40. Izban MG, Luse DS. The increment of SII-facilitated transcript cleavage varies dramatically between elongation competent and incompetent RNA polymerase II ternary complexes. J Biol Chem 1993; 268:12874-85; PMID:8509421
41. Zhang C, Yan H, Burton ZF. Combinatorial control of human RNA polymerase II (RNAP II) pausing and transcript cleavage by transcription factor IIF, hepatitis delta antigen, and stimulatory factor II. J Biol Chem 2003; 278:50101-11; PMID:14506279; http://dx.doi.org/10.1074/jbc.M307590200
42. Nielsen S, Zenkin N. Transcript assisted phosphodiester bond hydrolysis by eukaryotic RNA polymerase II. Transcription 2013; 4:4; PMID:24270513; http://dx.doi.org/10.4161/trns.27062
43. Chafin DR, Claussen TJ, Price DH. Identification and purification of a yeast protein that affects elongation by RNA polymerase II. J Biol Chem 1991; 266:9256-62; PMID:1851172
44. Izban MG, Luse DS. Factor-stimulated RNA polymerase II transcribes at physiological elongation rates on naked DNA but very poorly on chromatin templates. J Biol Chem 1992; 267:13647-55; PMID:1618865
45. Čabart P, Újvári A, Pal M, Luse DS. Transcription factor TFIIF is not required for initiation by RNA polymerase II, but it is essential to stabilize transcription factor TFIIB in early elongation complexes. Proc Natl Acad Sci U S A 2011; 108:15786-91; PMID:21896726; http://dx.doi.org/10.1073/pnas.1104591108
46. Khaperskyy DA, Ammerman ML, Majovski RC, Ponticelli AS. Functions of Saccharomyces cerevisiae TFIIF during transcription start site utilization. Mol Cell Biol 2008; 28:3757-66; PMID:18362165; http://dx.doi.org/10.1128/MCB.02272-07
47. Viktorovskaya OV, Engel KL, French SL, Cui P, Vandeventer PJ, Pavlovic EM, Beyer AL, Kaplan CD, Schneider DA. Divergent contributions of conserved active site residues to transcription by eukaryotic RNA polymerases I and II. Cell Rep 2013; 4:974-84; PMID:23994471; http://dx.doi.org/10.1016/j.celrep.2013.07.044
48. Derbyshire V, Grindley ND, Joyce CM. The 3′-5′ exonuclease of DNA polymerase I of Escherichia coli: contribution of each amino acid at the active site to the reaction. EMBO J 1991; 10:17-24; PMID:1989882
49. Sosunov V, Sosunova E, Mustaev A, Bass I, Nikiforov V, Goldfarb A. Unified two-metal mechanism of RNA synthesis and degradation by RNA polymerase. EMBO J 2003; 22:2234-44; PMID:12727889; http://dx.doi.org/10.1093/emboj/cdg193
50. Steitz TA, Smerdon SJ, Jäger J, Joyce CM. A unified polymerase mechanism for nonhomologous DNA and RNA polymerases. Science 1994; 266:2022-5; PMID:7528445; http://dx.doi.org/10.1126/science.7528445
51. Fishburn J, Hahn S. Architecture of the yeast RNA polymerase II open complex and regulation of activity by TFIIF. Mol Cell Biol 2012; 32:12-25; PMID:22025674; http://dx.doi.org/10.1128/MCB.06242-11
52. Pal M, Ponticelli AS, Luse DS. The role of the transcription bubble and TFIIB in promoter clearance by RNA polymerase II. Mol Cell 2005; 19:101-10; PMID:15989968; http://dx.doi.org/10.1016/j.molcel.2005.05.024
53. Krogan NJ, Kim M, Ahn SH, Zhong G, Kobor MS, Cagney G, Emili A, Shilatifard A, Buratowski S, Greenblatt JF. RNA polymerase II elongation factors of Saccharomyces cerevisiae: a targeted proteomics approach. Mol Cell Biol 2002; 22:6979-92; PMID:12242279; http://dx.doi.org/10.1128/MCB.22.20.6979-6992.2002
54. Cojocaru M, Jeronimo C, Forget D, Bouchard A, Bergeron D, Côte P, Poirier GG, Greenblatt J, Coulombe B. Genomic location of the human RNA polymerase II general machinery: evidence for a role of TFIIF and Rpb7 at both early and late stages of transcription. Biochem J 2008; 409:139-47; PMID:17848138; http://dx.doi.org/10.1042/BJ20070751
55. Pan G, Greenblatt J. Initiation of transcription by RNA polymerase II is limited by melting of the promoter DNA in the region immediately upstream of the initiation site. J Biol Chem 1994; 269:30101-4; PMID:7982911
56. Puig O, Caspary F, Rigaut G, Rutz B, Bouveret E, Bragado-Nilsson E, Wilm M, Séraphin B. The tandem affinity purification (TAP) method: a general procedure of protein complex purification. Methods 2001; 24:218-29; PMID:11403571; http://dx.doi.org/10.1006/meth.2001.1183
57. Liu X, Bushnell DA, Wang D, Calero G, Kornberg RD. Structure of an RNA polymerase II-TFIIB complex and the transcription initiation mechanism. Science 2010; 327:206-9; PMID:19965383; http://dx.doi.org/10.1126/science.1182015

58. Komissarova N, Kireeva ML, Becker J, Sidorenkov I, Kashlev M. Engineering of elongation complexes of bacterial and yeast RNA polymerases. Methods Enzymol 2003; 371:233-51; PMID:14712704; http://dx.doi.org/10.1016/S0076-6879(03)71017-9
59. Winston F, Dollard C, Ricupero-Hovasse SL. Construction of a set of convenient Saccharomyces cerevisiae strains that are isogenic to S288C. Yeast 1995; 11:53-5; PMID:7762301; http://dx.doi.org/10.1002/yea.320110107
60. Sikorski RS, Hieter P. A system of shuttle vectors and yeast host strains designed for efficient manipulation of DNA in Saccharomyces cerevisiae. Genetics 1989; 122:19-27; PMID:2659436
61. Boeke JD, Trueheart J, Natsoulis G, Fink GR. 5-Fluoroorotic acid as a selective agent in yeast molecular genetics. Methods Enzymol 1987; 154:164-75; PMID:3323810; http://dx.doi.org/10.1016/0076-6879(87)54076-9
62. Amberg DC, Burke DJ, Strathern JN. Methods in Yeast Genetics: A Cold Spring Harbor Laboratory Course Manual, 2005 Edition. Cold Spring Harbor, NY: Cold Spring Harbor Press, 2005.